Terrestrial long-baseline neutrino-oscillation experiments

Robert H. Bernstein and Stephen J. Parke
Fermi National Accelerator Laboratory, P.O. Box 500, Batavia, Illinois 60510
(Received 27 March 1991)

We present a systematic study of potential long-baseline (distances >300 km) neutrino-oscillation experiments performed with ν_μ and $\bar{\nu}_\mu$ beams from the Fermilab Main Injector ($<E_\nu>\approx$ 10–20 GeV). The effects of matter enhancement are included where appropriate. We find that there are three key variables for such an experiment: the length of the baseline, the muon energy threshold, and the minimum measurable oscillation probability. An advantage in one of these variables can easily be negated by a disadvantage in one of the others. Finally, for any long-baseline experiment at these energies to conclusively confirm or refute the interpretation of the atmospheric neutrino deficit as neutrino oscillations it must have a low energy threshold and a low minimum measurable oscillation probability.

I. INTRODUCTION

The recent indications of a deficit in the ν_μ flux of atmospheric neutrinos and the long-standing solar-neutrino problem have motivated new searches for neutrino oscillations with small neutrino Δm^2 (< 1 eV^2) [1]. The neutrino beams available from the Fermilab Main Injector [2] will provide a unique laboratory for the study of such effects. They will be intense, well-understood beams with neutrino energies from 10 to 50 GeV and by constructing experiments at large distances (hundreds of kilometers) the experiments can probe regions of parameter space relevant to these puzzles. One feature of such experiments is that the neutrino beams would pass through the Earth's crust, permitting matter enhancement to affect the oscillations. This paper addresses the physics accessible at such experiments. We first review the phenomenon of neutrino oscillations with an emphasis on matter enhancement; next we describe the likely experimental errors and conclude with a description of the potential power of such searches. We find that the ability of experiments to search for matter enhancement must include excellent systematic controls or these effects cannot be detected [3].

II. REVIEW OF NEUTRINO OSCILLATION PHENOMENOLOGY

A. Review of neutrino oscillations in vacuum

The time evolution of an ultrarelativistic plane-wave neutrino state propagating in a vacuum with momentum K in the mass-eigenstate basis is given by the trivial relation

$$|\nu(t)\rangle = \nu_1^0(t)\,|\nu_1^0\rangle + \nu_2^0(t)\,|\nu_2^0\rangle. \tag{2.1}$$

The Dirac equation for this state reduces to the Schrödinger-type equation

$$i\frac{d}{dt}\begin{pmatrix}\nu_1^0\\ \nu_2^0\end{pmatrix} = \begin{pmatrix}\sqrt{K^2+m_1^2} & 0\\ 0 & \sqrt{K^2+m_2^2}\end{pmatrix}\begin{pmatrix}\nu_1^0\\ \nu_2^0\end{pmatrix}. \tag{2.2}$$

In the ultrarelativistic limit we can use the approximation that

$$\sqrt{K^2+m_i^2} = \left(K+\frac{m_1^2+m_2^2}{4K}\right) \mp \frac{\Delta m_0^2}{4K} + \mathcal{O}\left(\frac{m^4}{K^3}\right), \tag{2.3}$$

where $\Delta m_0^2 \equiv m_2^2 - m_1^2$ and the minus (plus) sign is for the 1 (2) eigenstate. Notice that in this expression $[K+(m_1^2+m_2^2)/4K]$ is common to both mass eigenstates and can be removed by changing the overall phase of the neutrino state by an amount

$$\exp\left[i\left(K+\frac{m_1^2+m_2^2}{4K}\right)t\right]. \tag{2.4}$$

After this change of phase the time evolution is governed by

$$i\frac{d}{dt}\begin{pmatrix}\nu_1^0\\ \nu_2^0\end{pmatrix} = \frac{1}{2}\begin{pmatrix}-\frac{\Delta m_0^2}{2K} & 0\\ 0 & \frac{\Delta m_0^2}{2K}\end{pmatrix}\begin{pmatrix}\nu_1^0\\ \nu_2^0\end{pmatrix}. \tag{2.5}$$

In general the vacuum mass eigenstates are not identical to the flavor eigenstates but are related by

$$\begin{pmatrix}\nu_1^0\\ \nu_2^0\end{pmatrix} = \begin{pmatrix}\cos\theta_0 & \sin\theta_0\\ -\sin\theta_0 & \cos\theta_0\end{pmatrix}\begin{pmatrix}\nu_e\\ \nu_\mu\end{pmatrix}, \tag{2.6}$$

where θ_0 is the vacuum mixing angle. In this flavor basis the time evolution is

$$i\frac{d}{dt}\begin{pmatrix}\nu_e\\ \nu_\mu\end{pmatrix} = \frac{1}{2}\begin{pmatrix}-\frac{\Delta m_0^2}{2K}\cos 2\theta_0 & \frac{\Delta m_0^2}{2K}\sin 2\theta_0\\ \frac{\Delta m_0^2}{2K}\sin 2\theta_0 & \frac{\Delta m_0^2}{2K}\cos 2\theta_0\end{pmatrix}\begin{pmatrix}\nu_e\\ \nu_\mu\end{pmatrix}. \tag{2.7}$$

From Eqs. (2.5) and (2.6) it is easy to calculate the probability of producing one flavor of neutrino ν_a at the source, letting the neutrino propagate to the detector, a distance L away, and then detecting the neutrino as a different flavor ν_b. This transition probability is

 ©1991 The American Physical Society

$$\mathcal{P}_{ab} = \sin^2 2\theta_0 \sin^2\left(1.27\frac{\Delta m_0^2 L}{K}\right), \quad (2.8)$$

where Δm_0^2, K, and L are measured in eV^2, GeV, and kilometers, respectively (we use these units throughout). The experiments measure this probability and either measure a finite value for $\mathcal{P}_{ab}$ or assign a limit $\mathcal{P}_{ab} < \epsilon$; the value of ϵ, the neutrino energy spectrum, and the source-to-detector distance then define a region in the $(\sin^2 2\theta_0, \Delta m_0^2)$ plane for each experiment. This ϵ should be thought of as a minimum measurable oscillation probability for the experiment.

The size of ϵ, or the limit in our ability to measure $\mathcal{P}_{ab}$, arises from four sources (assuming the statistical errors are small compared to the systematic uncertainties): (1) the contamination of the beam with other neutrino species, (2) the fractional uncertainty in the neutrino flux calculations, (3) the knowledge of the experimental acceptance for the different neutrino species, and (4) backgrounds to the ν_b signal; we discuss these issues in Sec. II. Then for large Δm_0^2 an experiment can explore any

$$\sin^2 2\theta_0 \geq 2\,\epsilon. \quad (2.9)$$

The factor of two comes from averaging the $\sin^2(1.27\Delta m_0^2 L/K)$ term in Eq. (2.8).

For $\sin^2 2\theta_0 = 1$ the limit on the mass difference squared is

$$\Delta m_0^2 \geq \frac{\sqrt{\epsilon}}{1.27}\frac{K}{L}, \quad (2.10)$$

assuming $\epsilon << 1$. Note the momentum factor in the numerator as this will be important to us later. For smaller $\sin^2 2\theta_0$ a good *approximation* to the probability contour is a straight line with slope $-\frac{1}{2}$ in a log-log plot in the $(\sin^2 2\theta_0, \Delta m_0^2)$ plane until this line intersects the vertical line from Eq. (2.9). In Fig. 1 this region is shown for various values of L and ϵ keeping the neutrino momentum fixed at 20 GeV.

B. Neutrino oscillations in uniform matter

The effect of matter on the neutrino evolution is seen easily in the flavor basis. The electron neutrino can elastically forward scatter off the electrons in the matter through the charged-current interaction [4] whereas the muon neutrinos cannot. The term that must be added to the top diagonal element of the evolution matrix in Eq. (2.7) is [5]

$$+\sqrt{2}\,G_F\,N_e. \quad (2.11)$$

Once again it is convenient to make the diagonal elements of the evolution matrix equal in magnitude but opposite in sign by changing the overall phase of the neutrino state by

$$\exp\left(i\,\frac{G_F\,N_e\,t}{\sqrt{2}}\right). \quad (2.12)$$

Then the neutrino evolution equation becomes

$$i\frac{d}{dt}\begin{pmatrix}\nu_e\\ \nu_\mu\end{pmatrix} = \frac{1}{2}\begin{pmatrix}-\frac{\Delta m_0^2}{2K}\cos 2\theta_0 + \sqrt{2}G_F N_e & \frac{\Delta m_0^2}{2K}\sin 2\theta_0\\ \frac{\Delta m_0^2}{2K}\sin 2\theta_0 & \frac{\Delta m_0^2}{2K}\cos 2\theta_0 - \sqrt{2}G_F N_e\end{pmatrix}\begin{pmatrix}\nu_e\\ \nu_\mu\end{pmatrix}. \quad (2.13)$$

If N_e is a constant or simple function this evolution equation can be solved analytically; otherwise it must be integrated numerically.

For uniform matter the matter mass eigenstates are the natural basis. They are obtained by finding Δm_N^2 and θ_N such that

$$\frac{\Delta m_N^2}{2K}\cos 2\theta_N = \frac{\Delta m_0^2}{2K}\cos 2\theta_0 - \sqrt{2}G_F N_e,$$
$$\frac{\Delta m_N^2}{2K}\sin 2\theta_N = \frac{\Delta m_0^2}{2K}\sin 2\theta_0\,, \quad (2.14)$$

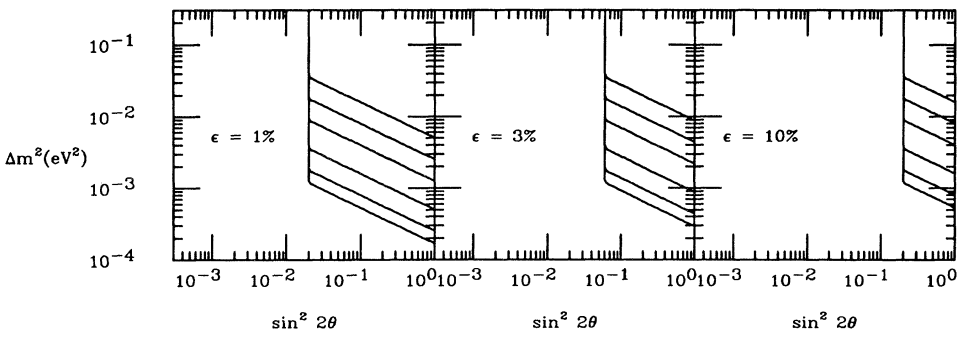

FIG. 1. The approximate range in the $(\sin^2 2\theta_0, \Delta m_0^2)$ plane for experiments in vacuum with ϵ = 1%, 3%, 10%, for distances of 300, 600, 1200, 3000, 6000, and 9000 km (from top to bottom) with a 20-GeV neutrino or antineutrino beam.

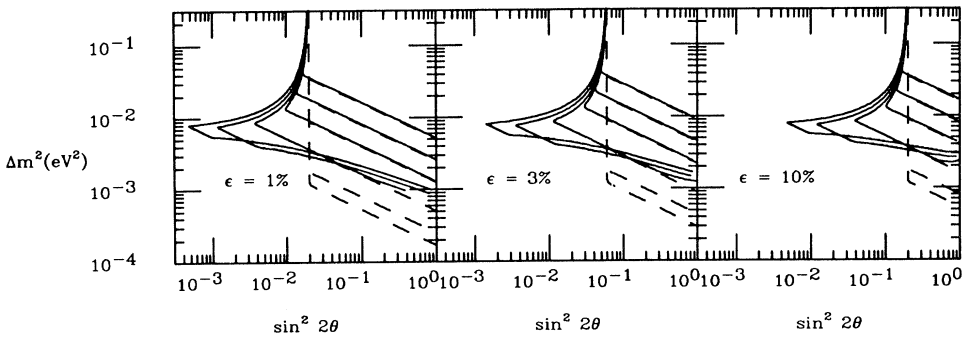

FIG. 2. The approximate range in the $(\sin^2 2\theta_0,\ \Delta m_0^2)$ plane for experiments in the Earth's crust (solid curve) with ϵ = 1%, 3%, 10%, for distances of 300, 600, 1200, 3000, 6000, and 9000 km (from top to bottom) with a 20-GeV neutrino beam. The dashed curves give the ranges in the $(\sin^2 2\theta_N,\ \Delta m_N^2)$ plane. Recall that the $(\sin^2 2\theta_N,\ \Delta m_N^2)$ contours are identical to the $(\sin^2 2\theta_0,\ \Delta m_0^2)$ contours for the corresponding vacuum experiment (the same L/E but no intervening matter).

where θ_N is the matter mixing angle that determines the matter mass eigenstates in terms of the flavor eigenstates:

$$\begin{pmatrix} \nu_1^N \\ \nu_2^N \end{pmatrix} = \begin{pmatrix} \cos\theta_N & \sin\theta_N \\ -\sin\theta_N & \cos\theta_N \end{pmatrix} \begin{pmatrix} \nu_e \\ \nu_\mu \end{pmatrix}. \tag{2.15}$$

The resonance density is the density which makes the diagonal elements of Eq. (2.13) zero and hence maximally mixes the two neutrino species

$$\theta_N = \frac{\pi}{4} \tag{2.16}$$

and

$$N_e = \frac{\Delta m_0^2 \cos 2\theta_0}{2K\sqrt{2}G_F}. \tag{2.17}$$

The time evolution in terms of these mass eigenstates is

$$i\frac{d}{dt}\begin{pmatrix} \nu_1^N \\ \nu_2^N \end{pmatrix} = \frac{1}{2}\begin{pmatrix} -\frac{\Delta m_N^2}{2K} & 0 \\ 0 & \frac{\Delta m_N^2}{2K} \end{pmatrix}\begin{pmatrix} \nu_1^N \\ \nu_2^N \end{pmatrix}. \tag{2.18}$$

From Eqs. (2.15) and (2.18) it is easy to see that the form of the transition probability is the same as before [Eq. (2.8)], but with the matter angles and matter mass difference squared replacing their vacuum values:

$$\mathcal{P}_{ab} = \sin^2 2\theta_N \sin^2\left(1.27\,\frac{\Delta m_N^2 L}{K}\right). \tag{2.19}$$

In terms of these matter parameters $(\sin^2 2\theta_N,\ \Delta m_N^2)$ the limits on the experiment are the same as before:

$$\sin^2 2\theta_N \geq 2\,\epsilon \tag{2.20}$$

and

$$\Delta m_N^2 \geq \frac{\sqrt{\epsilon}}{1.27}\frac{K}{L}. \tag{2.21}$$

In terms of the $(\sin^2 2\theta_0,\ \Delta m_0^2)$ plane we have to use Eq. (2.14) to make the transformation between the two. This is straightforward except in the case that $\cos 2\theta_N$ is negative. This occurs when the number density of electrons is larger than the resonance density of Eq. (2.17). In Figs. 2 and 3 the mapped regions for ν and $\bar{\nu}$ are shown together with the region explored in the vacuum for various detector distances, L, and limits on systematic uncertainties ϵ, for fixed momentum K = 20 GeV. The number density of electrons N_e is calculated using the average density times proton fraction for each chord in the Earth's mantle. The average density along the various chords used varies from 2.7 to 4.5 g cm^{-3} [6], but the root-mean-square variation is less than 15% of the

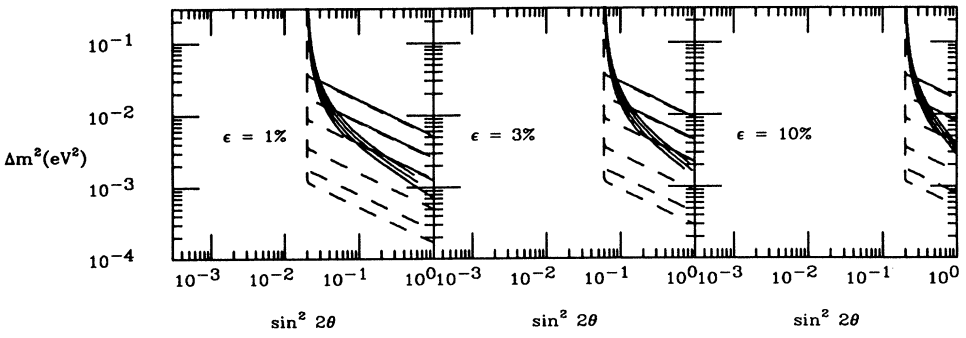

FIG. 3. The approximate range in the $(\sin^2 2\theta_0,\ \Delta m_0^2)$ plane for experiments in the Earth's crust (solid curve) with ϵ = 1%, 3%, 10%, for distances of 300, 600, 1200, 3000, 6000, and 9000 km with a 20-GeV antineutrino beam. For an explanation of the dashed curves, see Fig. 2.

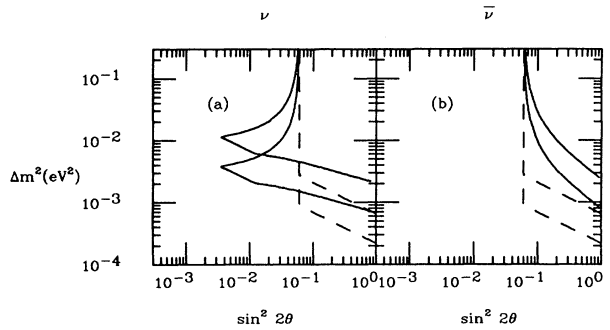

FIG. 4. The approximate range in the $(\sin^2 2\theta_0, \Delta m_0^2)$ plane for the following conditions: $L = 6000$ km and $\epsilon = 3\%$ with the energy of the beam $E = 30$ GeV (upper curve) and $E = 10$ GeV (lower curve), for (a) neutrinos and (b) antineutrinos, assuming $\Delta m_0^2 > 0$. For an explanation of the dashed curves, see Fig. 2.

average density for that chord. None of the chords used enter the Earth's core.

If we fix the detector distance L and the minimum measurable probability ϵ but vary the momentum K the plot is scaled up or down without any change in shape. This is because the bulge on the left of the plot is caused by the mass difference being close to the value needed for resonance

$$\Delta m_0^2 = \frac{2K\sqrt{2}G_F N_e}{\cos 2\theta_0}. \tag{2.22}$$

This Δm_0^2 scales with momentum in exactly the same way as does the minimum Δm_0^2 of Eq. (2.10). The size of the bulge is determined by the distance between the source and the detector and the number density of electrons in the mantle of the Earth. Figure 4(a) is an example of the same experiment with two different momenta for the neutrinos, all other variables held fixed.

C. Antineutrino-oscillation experiments in uniform matter

For antineutrinos propagating through matter, the situation is the same as for neutrinos but with

$$\sqrt{2}G_F N_e \longrightarrow -\sqrt{2}G_F N_e. \tag{2.23}$$

Figure 4(b) is the same as Fig. 4(a) except for antineutrinos instead of neutrinos. We have implicitly assumed Δm_0^2 is positive; if it is negative then the roles of neutrinos and antineutrinos are reversed.

III. EXPERIMENT

Oscillation experiments are one of two types: appearance or disappearance. Appearance experiments search for the presence of a particular species of neutrino where none was expected. Disappearance experiments measure the flux of a given species at two or more locations and search for a variation with L/E [7].

High-energy neutrino beams are generally $> 95\%$ ν_μ with a small admixture of ν_e. Hence appearance experiments at accelerators have concentrated on the oscillation $\nu_\mu \leftrightarrow \nu_e$ and disappearance experiments have studied $\nu_\mu \leftrightarrow \nu_X$. A ν_e appearance experiment requires a well-understood initial ν_e flux and detectors capable of precise detection and isolation of the ν_e component. The experiments have been limited to $P(\nu_\mu \leftrightarrow \nu_e) > 0.5\%$ by backgrounds to the ν_e signal and uncertainty in the initial flux.

Disappearance measurements from ν_μ use two detectors at different locations: the first detector measures the ν_μ flux in the beam. The observed rate in the upstream detector is then used to predict the rate in the second, downstream detector. After correcting for solid angle, acceptance, and other effects the experiment searches for a dependence of rate with L/E. Here the detectors need not be as complicated because muons, detected in both locations, are easier to identify than electrons. This class of experiments has been limited by the statistical error in the second detector; in order to reach an interesting range of L/E, the second detector must be well downstream of the first, but then the smaller solid angle of the second detector results in correspondingly fewer events.

No accelerator experiment, given the combination of experimental errors, beam energies, and distances, has been able to search for oscillations with $\Delta m^2 \lesssim 0.1$ eV^2; experiments at reactors have been able to reach $\Delta m_0^2 \approx 0.01$ eV^2, but only for large mixing angles [8].

The atmospheric neutrino deficit described earlier may indicate oscillations with either $\Delta m_{\mu e}^2 \sim 10^{-2\pm0.5}$ eV^2 or $\Delta m_{\mu\tau}^2 \sim 10^{-2\pm1}$ eV^2 with $\sin^2 2\theta > 0.2$ [9, 10]. This region of parameter space is up to an order of magnitude below existing searches. The evidence for oscillations presented by these experiments is not conclusive because of a variety of systematic errors; a well-understood beam with a known spectrum would be invaluable in confirming or refuting the idea that neutrino oscillations are responsible for the effects. This situation has motivated suggestions for experiments using the intense neutrino beams available at the Fermilab Main Injector [2, 11]. In order to reach the relevant region, the experiments must search at large L/E; hence the name "long baseline."

The Fermilab Main Injector neutrino beams will have energies of approximately 10–50 GeV with a mean of 16 GeV; a typical spectrum is displayed in Fig. 5. Values of L (baselines) of more than a few hundred kilometers are then required to map out the interesting region. In this paper, we choose two values of L motivated by a range of possible experiments: 600 and 6000 km. The Main Injector neutrino beam will yield approximately 800 events/kton yr for a detector with solid angle of 1 nsr; a one-year run at the Main Injector would provide 2×10^{20} protons [2].

A. Disappearance experiments

The suggested disappearance experiments will measure the initial ν_μ flux at some short distance (≈ 0.6 km) with high statistics and then remeasure it a distance L downstream. One interesting proposal is to use a proposed

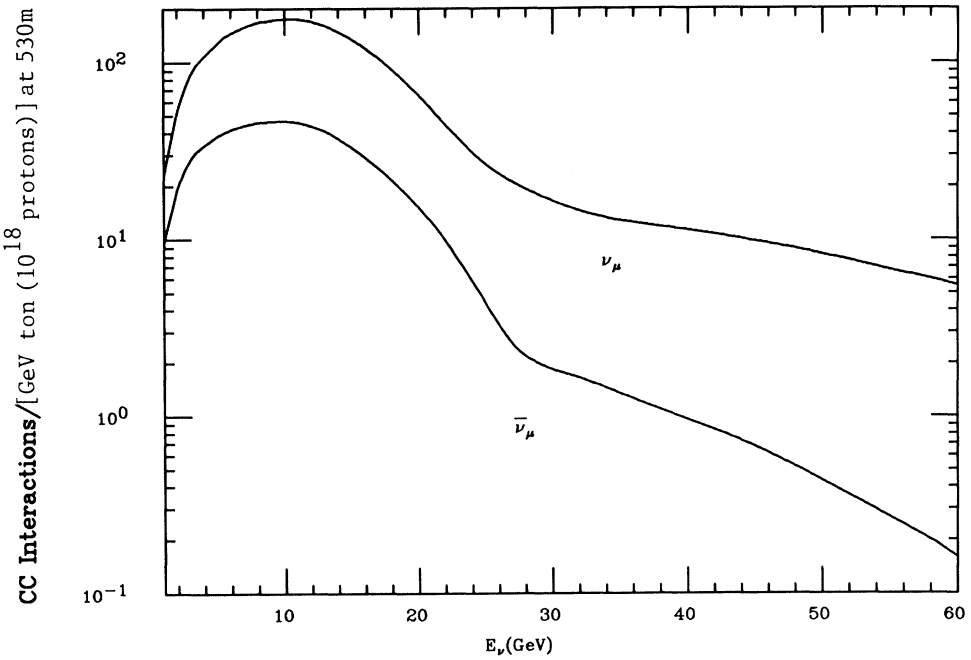

FIG. 5. The ν_μ and $\bar{\nu}_\mu$ spectra used in the calculation. The events have been weighted for the linearly rising neutrino and antineutrino cross sections. The incident proton energy at the Fermilab Main Injector is taken to be 120 GeV.

$\nu_\mu \leftrightarrow \nu_\tau$ search [12] as the near detector, combining a variety of oscillation experiments along one beam line; in this case, the errors on the initial measurement can probably be kept to $\pm 1\%$.

The second measurement, at the long-baseline detector itself, has a variety of systematic errors. We do not present an exhaustive list, but concentrate on those which we think will determine ϵ.

This class of experiments will form a ratio to give the change in muon-neutrino flux. The numerator is derived from the number of charged-current interactions taking place in the surrounding medium where the resulting muon passes through and triggers the detector; we denote the acceptance for these muons by A_μ. The ν_μ flux is then

$$f_{\nu_\mu} = \frac{N_\mu}{A_\mu} \tag{3.1}$$

and the systematic error is the error in the acceptance A_μ. The rate of ν_μ interactions in the upstream detector (which we take to have negligible error for simplicity) can then be used to predict the flux in the downstream detector to search for oscillations.

Measurements of the absolute flux of parent π's and K's in neutrino beams are typically no better than a few percent and are notoriously difficult to check. It is therefore unlikely that a signal for ν_μ disappearance could be established by comparing the observed ν_μ rate to the flux-normalized prediction. A measurement of $\nu_\mu \leftrightarrow \nu_e$ based on a prediction of the initial ν_e/ν_μ fraction could have significant systematic errors arising from errors in the simulation of the beam-defining train. The history of such experiments leads us to believe that an upstream detector which *simultaneously* measures the ν_μ flux and/or ν_e fraction is essential.

The value of A_μ and its energy dependence are functions of the individual experiment. The nature of the detector and of the surrounding medium will determine how well these acceptances can be understood. One important variable is the threshold energy for the detection of a muon; a large detector may require a correspondingly larger threshold energy unless the detector is densely instrumented.

Internal checks on the acceptance will be problematic because of the small statistical samples available. Depending on distance, between 100–6000 contained events/yr are expected in prototypical detectors and although the statistical limits on ϵ are good, the statistical limit on estimation of the systematic errors will be no better than 1–3%. The experiments normally quote 90% C.L exclusion contours, and so we choose a range of ϵ which reflect likely 90% C.L. limits. A limit of 1% seems the best which is ideally achievable given that neither the flux nor the acceptance error is expected to be smaller than 1%, and a reasonable worst-case error is $\epsilon = 10\%$ at 90% C.L. We have also chosen to present $\epsilon = 3\%$ as a "middle" value.

B. Appearance experiments

An appearance experiment is a far more convincing method of demonstrating neutrino oscillations than a disappearance measurement. We discuss below two possible modes for an appearance search.

First, the ability to distinguish ν_e from ν_μ neutral-current events would permit searches for $\nu_\mu \leftrightarrow \nu_e$ ap-

pearance. A combined appearance-disappearance signal in one experiment would be strong evidence for an oscillation signal. All of the suggested detectors are in principle capable of performing a $\nu_\mu \leftrightarrow \nu_e$ search but with less reach than in the disappearance channel. The experiments are difficult and require specialized apparatuses designed for such a signal. The technique has been studied in ν_e appearance searches at BNL [7]. One major source of error, which creates stringent demands on the detector, is π^0 production in the shower with subsequent e^+e^- pair production; either of the e^+e^- tracks can easily be confused with a ν_e charged-current signal. The other source of error, the ν_e contamination in the beam, will have been measured in the upstream detector, although extrapolation from the ν_e content at ≈ 600 m to the fraction at 600–6000 km will require a well-measured targeting angle and accurate geodesy.

It may also be that the most interesting channel is not $\nu_\mu \leftrightarrow \nu_e$ but $\nu_\mu \leftrightarrow \nu_\tau$. Small $\Delta m^2_{\mu\tau}$ values could explain the atmospheric neutrino deficit. Although matter enhancement plays no role in the $\nu_\mu \leftrightarrow \nu_\tau$ channel, the long baselines available permit searches for oscillations at small $\Delta m^2_{\mu\tau}$. Such an experiment would be an invaluable addition to $\nu_\mu \leftrightarrow \nu_\tau$ searches. A signal in this channel would be difficult to isolate, because the charged-current interaction $\nu_\tau N \rightarrow \tau X$, followed by the decay $\tau \rightarrow \mu\nu_\mu\nu_\tau$, would produce a muon difficult to distinguish from the muons resulting from the predominant $\nu_\mu N \rightarrow \mu X$ reaction.

An experiment capable of cleanly distinguishing charged- from neutral-current events could search for $\nu_\mu \leftrightarrow \nu_\tau$ oscillations through a deviation of the observed $R_\nu = \sigma(\nu_\mu, \mathrm{NC})/\sigma(\nu_\mu, \mathrm{CC})$ from the expected value. R_ν is currently known to $< 2.0\%$ and significant improvements are forthcoming from deep-inelastic measurements of $\sin^2\theta_W$ at Fermilab [13, 14]. The measurement of the numerator of R_ν would rely on τ decays into hadrons. These decays would look like neutral-current events, and hence will cause an increase in the ratio over that expected by standard model electroweak processes, signaling oscillations. A simultaneous measurement of R_ν in a smaller but otherwise identical upstream detector would remove many systematic difficulties and makes this a promising technique.

In order to determine the denominator $\sigma(\nu, \mathrm{CC})$, the experiment would detect charged-current interactions by observing the muon exiting from the hadronic shower; the detectors would need sufficient fiducial mass along the beam direction to absorb the shower and then detect the exiting muon. The analysis techniques have been carefully studied in measurements of R_ν at the Fermilab and CERN experiments [15, 16] and extrapolation to the lower energies (50–100 GeV neutrinos for the old experiments vs 10–20 GeV at the Main Injector) would be straightforward. Such an experiment would also have the significant advantage of forming f_{ν_μ} with solely contained events, where the knowledge of the acceptance and controls over systematic effects would be far greater than for interactions taking place in the surroundings.

IV. RESULTS AND CONCLUSIONS

A detailed evaluation of the systematic errors in long-baseline oscillation experiments is beyond the scope of this paper. Our approach has been to assume a probability ϵ and calculate the attainable limits; we hope this will stimulate the experiments to meet these levels and pro-

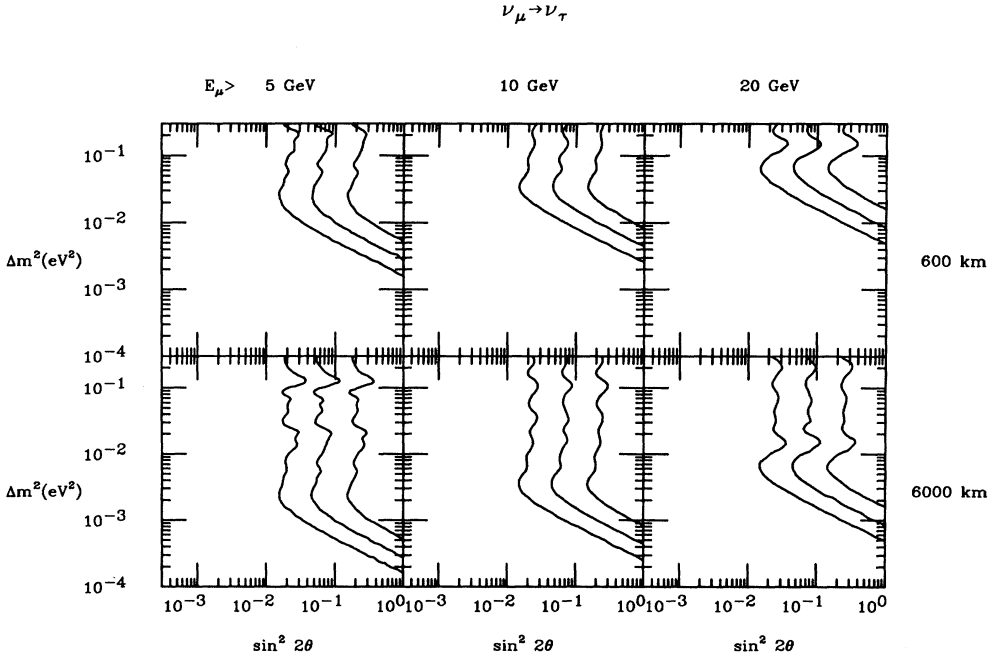

FIG. 6. The excluded region in the $(\sin^2 2\theta_0, \Delta m^2_0)$ plane for $\nu_\mu \leftrightarrow \nu_\tau$ for $L = 600$ and 6000 km with $\epsilon = 1$, 3, and 10% and muon-detection thresholds as shown.

vide a quantitative sense of the potential measurements of matter-enhanced oscillations [17].

We have calculated the limits with ν_μ and $\bar{\nu}_\mu$ spectra given in Fig. 5. The neutrinos and antineutrinos then produced muons through charged-current interactions using the appropriate y distribution for deep-inelastic scattering [18].

The acceptance for muons is a complicated and experiment-dependent quantity. We modeled it with a θ function; if the muon energy was less than 5, 10, or 20 GeV (each of three cases) the muon was considered lost; for energies greater than the appropriate value the acceptance was assumed perfect. The neutrinos oscillated according to Eq. (2.13) and a grid of probabilities was then calculated, leading to the contours. We have included the effects of the varying density of the Earth by integrating this equation over the chords of interest; $\Delta\rho/\rho < 15\%$ and the effects are small [6].

We first present the results for $\nu_\mu \leftrightarrow \nu_\tau$ oscillations. Since these oscillations are unaffected by matter enhancement, the contours scale in a simple way. We plot $\nu_\mu \leftrightarrow \nu_\tau$ contours at 600 and 6000 km for $\epsilon = 1\%$, 3%, and 10% in Figs. 6 and 7 for neutrinos and antineutrinos, respectively. These figures are very similar but differ slightly due to different spectra and y distributions for the neutrinos and antineutrinos.

The results for $\nu_\mu \leftrightarrow \nu_e$ oscillations at 600 and 6000 km are shown in Fig. 8 for neutrinos and Fig. 9 for antineutrinos. We see immediately that for a given experiment the region of sensitivity is enlarged due to matter enhancement for neutrinos and reduced by matter enhancement for antineutrinos. Both of these effects could be investigated in an appropriate experiment. However, the statistics of an antineutrino run would suffer from the smaller cross section ($\sigma_{\bar{\nu}}/\sigma_\nu \approx 0.5$) and from a less intense $\bar{\nu}_\mu$ beam; hence an antineutrino experiment would need to run for six times as long as its neutrino counterpart to achieve the same statistical power.

Finally, the region of sensitivity of any long-baseline experiment could be greatly reduced by increased systematic errors and/or higher energy thresholds. As an example of this, we have compared two idealized experiments in Fig. 10 which differ only in their distance from the source. We vary systematics and energy thresholds to determine the sensitivity vs distance for the possible oscillation modes $\nu_\mu \leftrightarrow \nu_\tau$, $\nu_\mu \leftrightarrow \nu_e$, and $\bar{\nu}_\mu \leftrightarrow \bar{\nu}_e$ ($\bar{\nu}_\mu \leftrightarrow \bar{\nu}_\tau$ would be almost identical to $\nu_\mu \leftrightarrow \nu_\tau$). The solid and dotted-dashed curves show the neutrino-oscillation contours for 600- and 6000-km experiments where both have a 5-GeV muon energy threshold and $\epsilon = 1\%$. The 6000-km experiment has an extra region of accessible parameter space for $\nu_\mu \leftrightarrow \nu_\tau$, $\bar{\nu}_\mu \leftrightarrow \bar{\nu}_\tau$, and $\nu_\mu \leftrightarrow \nu_e$ arising from the greater distance and matter-enhanced oscillations. For $\bar{\nu}_\mu \leftrightarrow \bar{\nu}_e$ oscillations matter enhancement reduces the region of sensitivity and thus the advantage of the 6000-km experiment is marginal in this channel.

The above discussion assumes that the systematic effects would be independent of L. However, as we have argued, the systematic errors and thresholds are likely to be worse for the longer-baseline experiment. The dashed contours of Fig. 10 show the regions for a 6000-km experiment with a 10-GeV muon detection and threshold

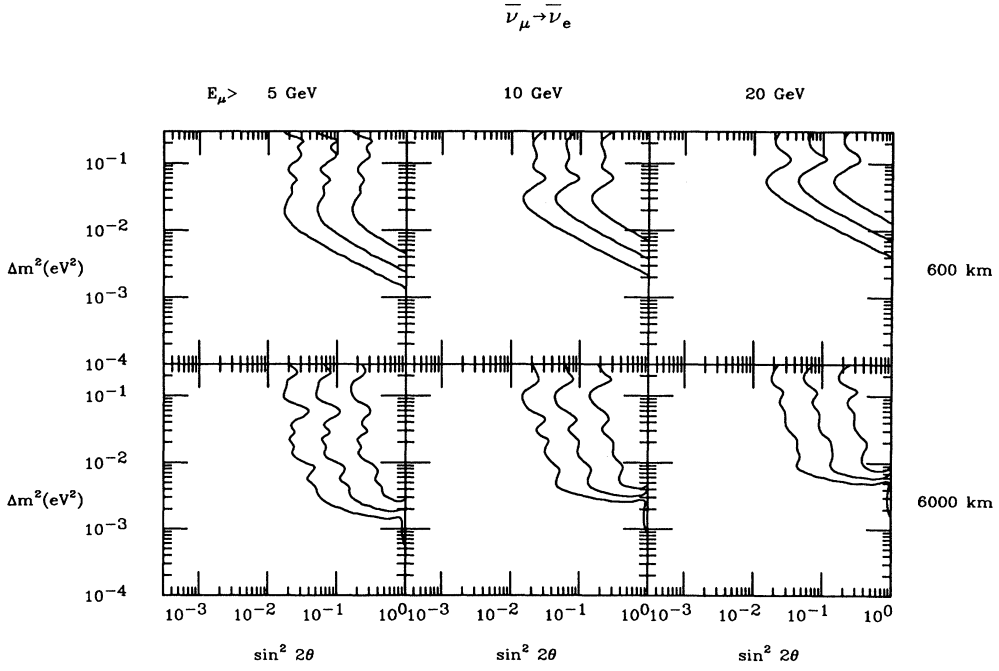

FIG. 9. The exclusion region in the $(\sin^2 2\theta_0, \Delta m_0^2)$ plane for $\bar{\nu}_\mu \leftrightarrow \bar{\nu}_e$ oscillations in the Earth for $L = 600$ and 6000 km with $\epsilon = 1$, 3, and 10% and muon-detection thresholds as shown.

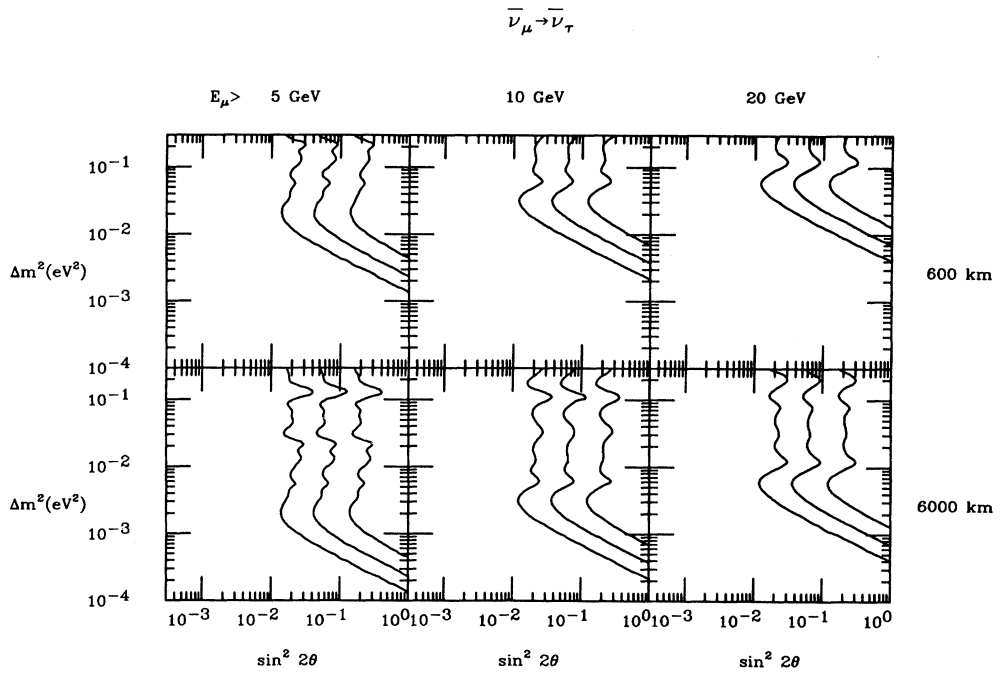

FIG. 7. The excluded region in the $(\sin^2 2\theta_0,\ \Delta m_0^2)$ plane for $\bar{\nu}_\mu \leftrightarrow \bar{\nu}_\tau$ for $L = 600$ and 6000 km with $\epsilon = 1$, 3, and 10% and muon-detection thresholds as shown. This plot is marginally different from Fig. 6 because of the different y distributions and spectra for neutrinos and antineutrinos.

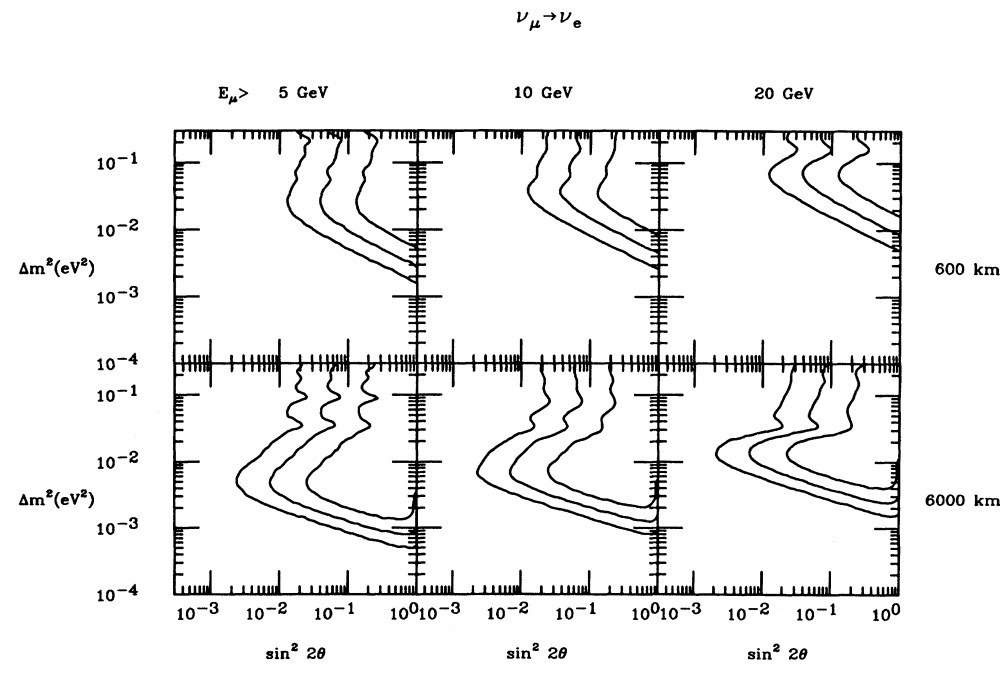

FIG. 8. The exclusion region in the $(\sin^2 2\theta_0,\ \Delta m_0^2)$ plane for $\nu_\mu \leftrightarrow \nu_e$ oscillations in the Earth for $L = 600$ and 6000 km with $\epsilon = 1$, 3, and 10% and muon-detection thresholds as shown.

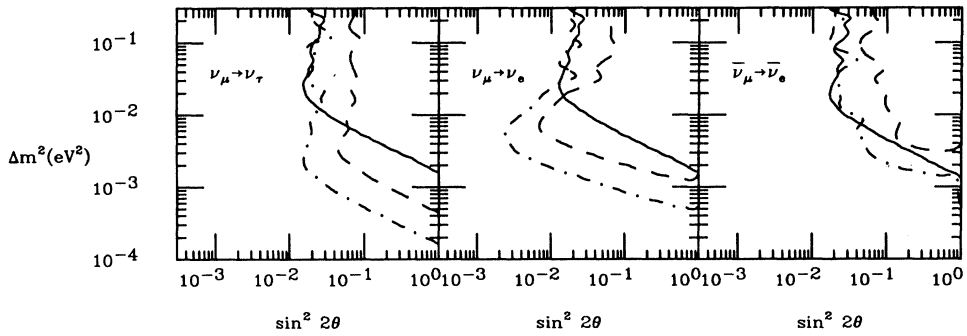

FIG. 10. Comparison of oscillation experiments with different baselines, muon-detection thresholds, and ϵ for the oscillation modes as indicated. The solid curve has parameters (600 km, 5 GeV, 1%), the dotted-dashed curve is (6000 km, 5 GeV, 1%), and the dashed curve is (6000 km, 10 GeV, 3%).

and $\epsilon = 3\%$. Now the advantages of the longer-baseline experiment are clearly reduced. In addition, the statistical errors of the 6000-km experiment would be much larger than the same experiment at 600 km. The change in solid angle would reduce the data sample by a factor of approximately 100, yielding no more than ≈ 8 events/kton yr; to ensure an equal statistical sample, a larger detector and/or a proportionately longer running time are required. Hence any long-baseline oscillation experiment must have low-energy detection thresholds as well as overcome both statistical *and* systematic barriers to be successful. While such difficulties could undoubtedly be managed, they present formidable experimental hurdles.

ACKNOWLEDGMENTS

We would like to thank W. Gajewski, M. C. Goodman, and M. Webster for valuable discussions. This work was supported by the U.S. Department of Energy under Contract No. DE-AC02-76CHO3000.

[1] K. S. Hirata *et al.*, Phys. Lett. B **205**, 416 (1988); T. Kajita, in *Proceedings of the XXVth International Conference on High Energy Physics*, Singapore, 1990, edited by K. K. Phua and Y. Yamaguchi (World Scientific, Singapore, 1991); D. Casper *et al.*, Phys. Rev. Lett. **66**, 2561 (1991); Ch. Berger *et al.*, Phys. Lett. B **245**, 305 (1990); **227**, 489 (1989); M. Aglietta *et al.*, Europhys. Lett. **8**, 611 (1989); M. Takita, Ph.D. thesis, University of Tokyo, 1989; R. Davis *et al.*, Phys. Rev. Lett. **20**, 1205 (1968).

[2] Conceptual Design Report: The Fermilab Main Injector, Rev. 2.3, Fermilab, Batavia, Illinois, 1990 (unpublished); R. Bernstein *et al.*, Conceptual Design Report: Neutrino Physics after the Main Injector Upgrade, Fermilab, Batavia, Illinois, 1991 (unpublished).

[3] A similar study, but more oriented toward the DUMAND detector, has been made by J. Pantaleone, Phys. Lett. B **246**, 245 (1990).

[4] There is also a flavor-diagonal contribution from the neutral-current interaction which can be removed by an overall phase change.

[5] L. Wolfenstein, Phys. Rev. D **17**, 2369 (1978).

[6] See, for example, F. D. Stacey, *Physics of the Earth* (Wiley, New York, 1969).

[7] For a general review of oscillation results, see M. Shaevitz, in *New Directions in Neutrino Physics at Fermilab*, Proceedings, Batavia, Illinois, 1988, edited by R. Bernstein (Fermilab, Batavia, 1988); a review of several neutrino-oscillation experiments with considerable detail on the experimental uncertainties can be found in *Opportunities for Neutrino Physics at BNL*, Proceedings of the Workshop, Upton, New York, 1987, edited by M. Murtagh (BNL Report No. 52079, Upton, 1987). Published results can be found in B. Blumenfeld *et al.*, Phys. Rev. Lett. **62**, 2237 (1989); L. A. Ahrens *et al.*, Phys. Rev. D **31**, 2732 (1985).

[8] V. Zacek *et al.*, Phys. Lett. **164B**, 193 (1985).

[9] K. Nakamura, in *Proceedings of the XXVth International Conference on High Energy Physics* (Ref. [1]).

[10] J. Learned, S. Pakvasa, and T. Weiler, Phys. Lett. B **207**, 79 (1988).

[11] K. Kodama *et al.*, Muon Neutrino to Tau Neutrino Oscillations, Fermilab Proposal P–803 (unpublished); W. Gajewski *et al.*, A Proposal for a Long Baseline Oscillation Experiment Using a High Intensity Neutrino Beam from the Fermilab Main Injector to the IMB Water Cerenkov Detector, Fermilab Proposal P–805 (unpublished); W. Allison *et al.*, A Long Baseline Neutrino Oscillation Experiment Using Soudan 2, Fermilab Proposal P–822 (unpublished); DUMAND–II Collaboration, A Terrestrial Long-Baseline Neutrino Oscillation Experiment using the Proposed Fermilab Main Injector and the DUMAND Detector, Fermilab Proposal P–824 (unpublished).

[12] K. Kodama (Ref. [11]).

[13] R. Bernstein, in Proceedings of Snowmass '90, Snowmass, CO, edited by R. Brock and H. Montgomery (to be published); T. Bolton *et al.*, Precision Measurements of Neutrino Neutral Currents Using a Sign-Selected Beam, Fermilab Proposal P–815 (unpublished).

[14] R. Brock, in *The Rice Meeting*, Proceedings of the Annual Meeting of the Division of Particles at Fields of the APS, Houston, Texas, 1990, edited by B. Bonner and H.

Miettinen (World Scientific, Singapore, 1990), p. 435.
[15] P. Reutens *et al.*, Phys. Lett. **152B**, 404 (1985).
[16] A. Blondel *et al.*, Z. Phys. C **45**, 361 (1990).
[17] Disappearance experiments have a cutoff at large Δm^2 which would for the experiments considered here appear at $\approx$ 30–50 eV^2, well above the curves presented in this paper. If the distance from the source to the first detector L_1 is such that $1.27\Delta m^2 L_1/E \gtrsim \pi$, then the finite energy resolution of the detector will make it impossible to measure the phase of the oscillation. As an extreme case, consider $\Delta m^2 \gg E/L_1$; then the neutrinos are "fully mixed" and no further difference will be observed in a downstream detector. However, since the oscillations at large Δm^2 have already been excluded in previous appearance experiments, the upper limit is only relevant for the case of oscillations into a sterile neutrino.
[18] The structure functions were obtained by the CCFR Collaboration. See E. Oltman, Nevis Pub. No. 270, Ph.D. thesis.